Ji-Hong Li[a,b]
Mark J. Guiltinan[a]
Donald B. Thompson[b]

[a] The Huck Institutes of the Life Sciences, The Pennsylvania State University, University Park, PA 16802, USA
[b] Department of Food Science, The Pennsylvania State University, University Park, PA 16802, USA

The Use of Laser Differential Interference Contrast Microscopy for the Characterization of Starch Granule Ring Structure

A laser differential interference contrast (DIC) microscopy protocol was developed for the visualization of starch growth rings in an optical section series. Potato and maize starches were observed with this new technique. Partial lintnerization was necessary to visualize the rings. The best image contrast was obtained using a blue laser and image deconvolution. For native starches, growth rings were evident in potato starch, but not as much as in native normal and waxy maize starches. Lintnerization enhanced the visualization of growth rings until granule integrity became compromised (by 48 h for waxy maize and by 96 h for normal maize and potato starches). Density of growth rings was not different for normal and waxy maize starches (11.3 and 12.1 rings/10 μm) but was lower for potato starch (7.5 rings/10 μm). Compared to other techniques for visualization of growth rings such as SEM and TEM, this protocol is fast and simple with minimum sample preparation and little possibility of artifacts.

Keywords: DIC microscopy; Starch growth rings; Linterization

1 Introduction

Microscopy is an important visualization tool to characterize the morphology and internal structure of starch granules. Among microscopic techniques, bright field microscopy is commonly used to study aspects of starch granule morphology such as granule shape, granule size and size distribution, morphological changes during gelatinization, and acid and enzyme hydrolysis [1, 2]. Scanning electron microscopy (SEM) has been extensively used to study not only starch granule morphology but also granule ultrastructure after fracture or partial hydrolysis [3, 4]. SEM normally requires coating with heavy metals (e.g.; gold) to decrease sample charging and improve image quality. Transmission electron microscopy (TEM) has been used for ultrastructural study of starch granules [3–6]. This technique involves a complex multistep preparation including fixation, staining, washing, dehydration, embedding, and sectioning steps, which may introduce artifacts. Atomic force microscopy (AFM) is a relatively new technique to study starch granule surface features (topography) [7–9] and internal structure [10, 11] on a small total sampling area. Confocal laser scanning microscopy (CLSM) has been used as an advanced light microscopic technique for three-dimensional visualization of starch granules, granule channels, cavities inside starch granules, and the reaction between starch and other components [12–16]. However, fluorescent staining of optical sections using CLSM does not reveal the so-called "growth rings." Thus, each microscopic technique allows visualization of different starch structural features, and each has its own advantages and limitations.

Differential interference contrast (DIC) microscopy was introduced in the mid-1960s after the method was described by *Nomarski* in 1952. It is now widely used for biological research to study live cells and tissues [17]. In a standard configuration, a DIC microscope contains a pair of polarizing elements (a polarizer and an analyzer) and two crystalline beam-splitting devices (termed modified Wollaston prisms) for detecting gradients in optical path length within specimens and converting them into light intensity differences [17]. A light beam passes through a polarizer, producing a beam of linearly polarized light in the same plane, just as in polarized light microscopy. When the polarized light beam enters a Wollaston prism, each incident ray is split into two spatially separated parallel rays, named ordinary and extraordinary rays, vibrating at 90° relative to each other. The dual beams of parallel rays are then focused by a condenser lens and travel through a transparent specimen. In any part of the specimen in which adjacent regions differ either in refractive index or thickness, the two beams of rays are delayed or refracted differently resulting in slight optical path difference and a shift in phase. When recombined into elliptically polarized light by a second prism after the objective

Correspondence: *Donald B. Thompson*, Department of Food Science, 114 Borland Laboratory, The Pennsylvania State University, University Park, PA 16802, USA. Phone: +1-814-863-0481, Fax: +1-814-863-6132, e-mail: dbt1@psu.edu.

lens, these phase-shifted paired rays partially pass through the second polarizer, and subsequently generate an amplitude image of the specimen through interference at the image plane. Therefore, the difference in optical path is translated into a change in amplitude visualized as intensity in the final image observed in the eyepieces or captured by a digital video imaging system [17]. What is visualized by confocal DIC microscopy when the depth of focus is narrow is a virtual slice (an optical section) of the specimen, but without the need for fluorescent labeling, as commonly required in CLSM. This application of DIC microscopy for starch ultrastructure analysis has not been reported.

Starch is synthesized in plants as granules with characteristic size and shape that varies according to the plant source. Thus, the source of starch is commonly identified from its microscopic features [18]. However, not all starches can be easily identified based on external starch morphology. A convenient microscopic technique to explore aspects of granule ultrastructure (e.g., granule, growth rings, lamellae/crystallites, helices and molecules) would be useful. The objective of this study was to develop a protocol to apply laser DIC microscopy in the characterization of the internal structure of starch granules. We used this protocol to try to distinguish among growth ring patterns for maize and potato starches.

2 Materials and Methods

2.1 Starch sources

Normal maize starch (Melojel®) and waxy maize starch (Amioca®) were obtained from National Starch Co. (Bridgewater, NJ). Potato starch (S-4251) was purchased from Sigma Chemical Co. (St. Louis, MO).

2.2 Lintnerization of starch

Starch treated with hydrochloric acid (2.2 M, v/v) is referred to as lintnerized starch. A 50 mg starch sample was hydrolyzed with 2 mL, 2.2 M aqueous HCl at 37°C for up to 4 days in a shaking water bath. A 0.4 mL sample of the partially hydrolyzed suspension was taken at 12, 24, 48, and 96 h, then centrifuged (Eppendorf Centrifuge 5415C) at 2000 × *g* for 3 min and washed three times with deionized water. Finally, the volume of each sample was adjusted with deionized water to 0.2 mL for microscopic examination. Starch suspensions without acid hydrolysis (10 mg in 0.2 mL water hydrated for 30 min) were used as control (0 h hydrolysis). All starch hydrolyses were performed in duplicate.

2.3 Laser differential interference contrast microscopy

After vortexing, a 5 μL portion of starch suspension was immediately placed on a slide and covered by a cover slip. The starch preparations were visualized within 5 min using a confocal laser scanning microscopic system (Olympus Fluoview 300, Olympus America Inc., Melville, NY). The microscopic system consisted of an IX70 microscope with differential interference contrast optics, a laser source, confocal scanning, and a monitor. A blue argon laser was set to excitation wavelength of 488 nm and a red helium-neon laser was set to excitation wavelength of 633 nm. Because it led to better resolution, the blue laser was used for much of this study. A starch granule from a non-clumpy area of the slide was randomly selected. Focus was determined based on what gave the maximum contrast in the plane, using an objective PlanApo 60X/1.4 oil and an optical zoom (up to 10 × magnification). The settings were as follows: three-dimension (*x*-*y*-*z*) scanning mode, imaging rates of 3 frames/s, 512 × 512 pixel array size, and image depth resolution of 4096 gray levels (12-bit). With these settings, *x*, *y*-resolution is 0.24 μm and *z*-resolution is 0.28 μm according to the instrument configuration from the manufacturer. Sequential images of 20 optical sections per granule were taken at a continuous step size of 0.25 μm. For calculation of ring density, about 25 starch granules from each sample were photographed. Images were processed using deconvolution software (AutoDeblur and AutoVisualization Version 9.1, AutoQuant Imaging Inc., Waterliet, NY) to remove out-of-focus haze and blur from stacks of optical slide/sections. The brightness and darkness were adjusted using Adobe Photoshop CS software. Quantification of ring structure of starch granules was performed using analytical software of Fluoview and Image-Pro Plus (version 5.0, Media Cybernetics Inc., Silver Spring, MD). Density of granule rings was defined as the average number of rings per 10 μm along the long radius from the granule hilum to the exterior.

3 Results and Discussion

3.1 Effect of light source

Differential Interference Contrast micrographs of native and lintnerized starches were constructed using blue laser, red laser and normal bright light. Laser light is monochromatic and coherent (single-phase), and consists of directional waves with strong intensity, whereas normal bright light is a range of diffuse (non-coherent) wave lengths (400–750 nm) with weak intensity. Intense illumination with narrow and shorter wavelength generally results in higher image resolution. Fig. 1 shows the structure of an optical section of the same granule revealed using the blue and the red laser. Alternate dark and light

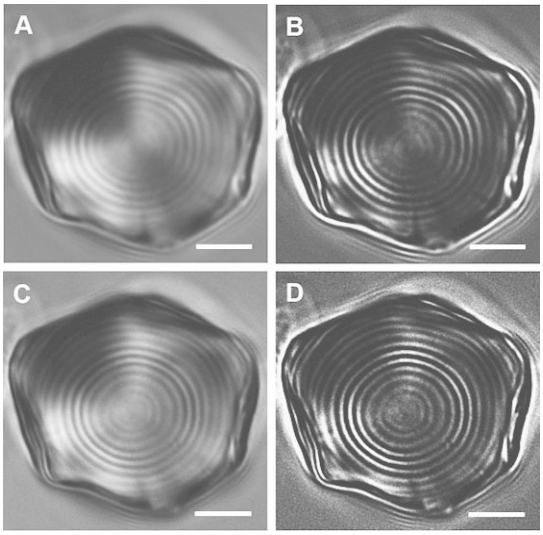

Fig. 1. Laser DIC micrographs of an optical section from a lintnerized normal maize starch granule hydrolyzed for 24 h at 37°C using red (A and B) and blue laser (C and D). A and C, before deconvolution; B and D, after deconvolution. Scale bar = 5 μm.

rings showed a symmetrical ring pattern. The blue laser revealed clearer granule internal structure with less blurring (Fig. 1 C) than either red laser (Fig. 1 A) or normal light (data not shown). The blue laser was used for subsequent visualization.

3.2 Image deconvolution

Image deconvolution is a computational technique to improve the contrast and resolution of digital images obtained. A suite of methods are designed to remove or reverse the out-of-focus blurring [19]. Individual images and those collected from a series of optical sections are suitable for improvement by deconvolution. The laser DIC micrographs of an optical section of a granule from lintnerized normal maize starch with and without deconvolution analysis are shown in Fig. 1. Compared to the original image (Fig. 1 A, C), the deconvolved image (Fig. 1 B, D) more clearly revealed the internal ring structure of the starch granule. The contrast of the deconvolved image using the blue laser (Fig. 1 D) was also better than that using the red laser (Fig. 1 B). Consequently this deconvolution method was applied for subsequent images reported below.

3.3 Optical sectioning

The optical sectioning ability of the DIC system enables high-resolution images to be obtained from focal planes, effectively allowing visualization of thin sections, within a relatively thick specimen. Laser DIC micrographs of an optical section series of a single lintnerized starch granule from normal maize starch at the step size of 1.25 μm are shown in Fig. 2. The optical sections were focused at each step size and the thickness of the optical section is limited by the *z*-resolution. The diameter of the section increased from the two uppermost section planes (*z*=1, *z*=2) to the central section planes (*z*=3–6). The central section planes showed a constant ring density in the central region of the granule. Our interpretation is schematically illustrated in Fig. 3, indicating a continuous internal ring structure within starch granules. Although some interference pattern outside granules is evident, the rings internal to the granule are either only evident after acid hydrolysis (for maize) or highly asymmetrical (for potato). Thus these rings are not artefactual. Moreover, the growth rings for normal maize starch bear a striking resemblance to those described by *Ridout* et al. [20] for lightly iodine-stained maize starch that is physically sectioned. One advantage of laser DIC microscopy compared to CLSM is that there is no photo-bleaching (rapid loss of fluorescent signal with time) effect during the observation for developing stacks of images by series sectioning.

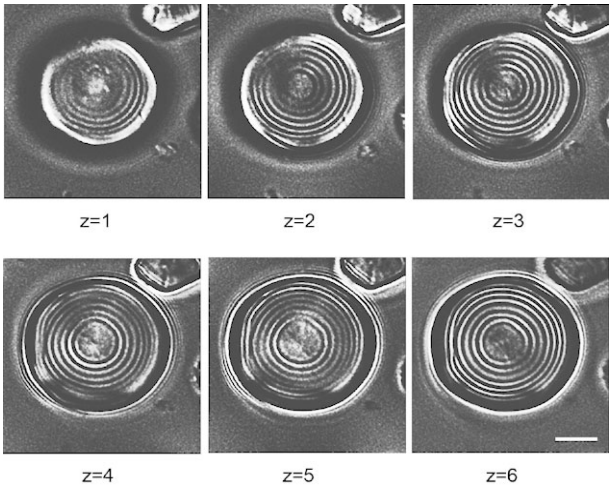

Fig. 2. Laser DIC micrographs of optical section series (at *z*-step size of 1.25 μm) of a single lintnerized normal maize starch granule hydrolyzed for 24 h at 37°C. Scale bar = 5 μm.

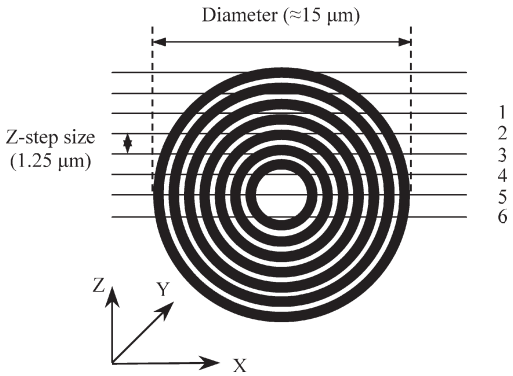

Fig. 3. Schematic optical sectioning of a single starch granule by a laser DIC microscopy. The position of sections from1 to 6 corresponded to *z*=1 to *z*=6 in Fig. 2.

3.4 Laser DIC microscopy of native starches

In the laser DIC micrographs of native maize starch granules, growth rings around the hilum were not clearly observed; however, a central cavity with internal channels/cracks was frequently observed (labeled as arrows in Fig. 4 C, E). For native potato starch granules, a number of layers of ring structure around the hilum and polarized crosses were evident even in the native starches (Fig. 4 A). Symmetrical rings were often off center for potato granules and ring density was highly variable with granule direction (Fig. 4 A). There is little evidence of rings for the native maize starches.

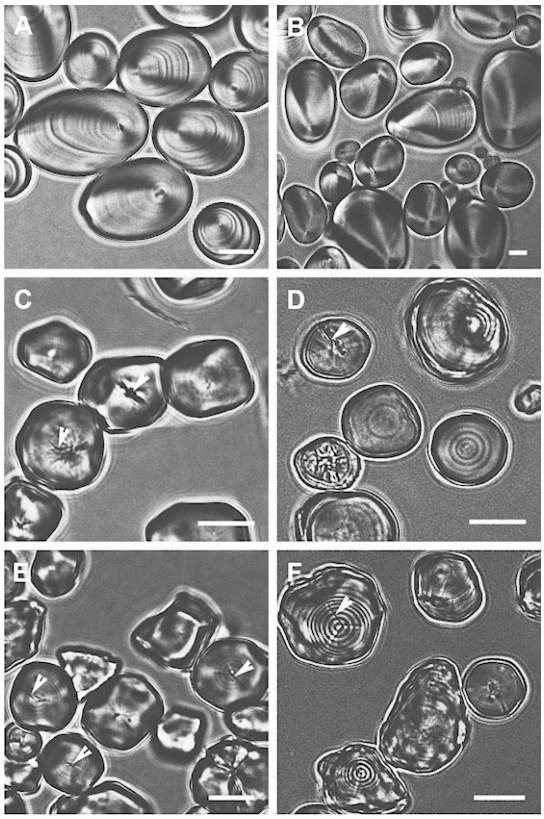

Fig. 4. Laser DIC micrographs of native (A, C, E) and lintnerized starch granules hydrolyzed for 12 h at 37°C (B, D, F). A and B, potato starch; C and D, normal maize starch; E and F, waxy maize starch. Scale bar = 10 μm. Arrows indicate central cavity with internal channels/cracks. Note: The scale was chosen to illustrate structural variation among granules.

3.5 Laser DIC microscopy of lintnerized starches

Acid causes scission of the most susceptible glucosidic linkages of starch. A mild acid hydrolysis is introduced to remove the amorphous and poorly crystalline regions of the granule without substantially changing the granular shape. The hydrolysis pattern, extent, and rate of hydrolysis depend on starch origin, acid type and concentration, and hydrolysis duration [21, 22].

Ring structures were evident in the central region of all the starch granules at 12 h hydrolysis (Fig. 4 B, D, F); at 24 h and 48 h hydrolysis, rings were apparent increasingly closer to the granule periphery (Fig. 5), indicating that the central region of the granule may be most susceptible to acid attack, perhaps because it is least well organized at the molecular level. At 96 h hydrolysis (data not shown), residual granules rapidly fragmented or cracked during observation, most likely due to increased fragility of the granules because of the removal of the more ductile connecting amorphous zones.

The hydrolysis pattern differed between potato and maize starches (Fig. 5). A number of main layers of ring structure with sub-layers around the hilum were more clear in potato starch granules at 24 h to 48 h hydrolysis (Fig. 5 A, B) than at 12 h hydrolysis (Fig. 4 B) and fragmented into several layers with rings after 96 h hydrolysis under the

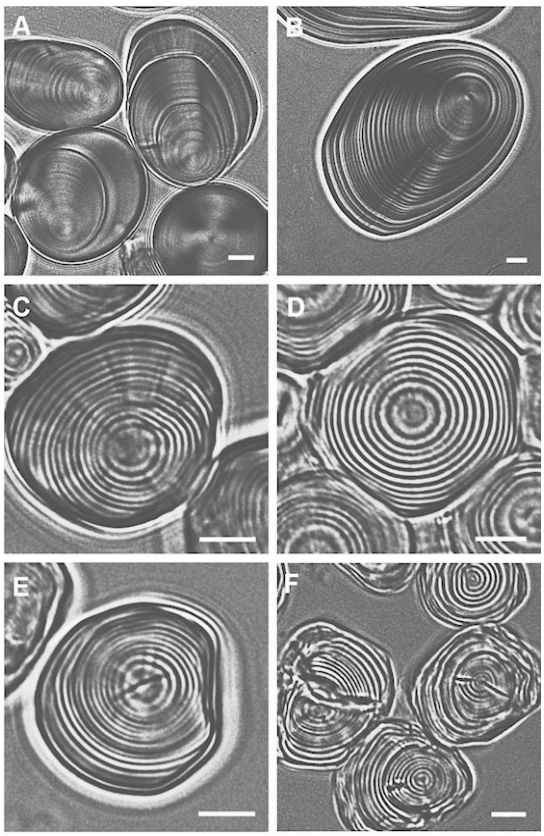

Fig. 5. Laser DIC micrographs of lintnerized starch granules hydrolyzed for 24 h (A, C, E) and 48 h (B, D, F) at 37°C. A and B, potato starch; C and D, normal maize starch; E and F, waxy maize starch. Scale bar = 5 μm. Note: After treatment, little variation was observed among granules. The scale was chosen to show granule detail.

high-intensity laser beam (data not shown). In normal maize and waxy maize starch, the hydrolysis started from the central region of the granule toward the periphery region of the starch granules indicated by increasing ring density (Fig. 5 C, D, E, F), but the hydrolysis of waxy starch seemed to be faster than that of normal maize starch and frequently resulted in cracks crossing the central region of the granule (Fig. 5 F). At 48 h hydrolysis, the granule integrity of the waxy maize starch appeared compromised.

3.6 Quantification of ring structure

Density of rings (defined as the number of visible rings per 10 μm along the maximum granule radius from the hilum) was measured when granule rings were clearly visualized and granules were mechanically intact (24–48 h hydrolysis). Potato starch granules had a lower ring density (7.5 ± 1.2) than did maize starch granules at the same length of radius. Ring density in waxy maize (12.1 ± 1.6) was similar to that in normal maize starches (11.3 ± 1.6).

4 Conclusions

In combination with acid hydrolysis, laser DIC microscopy may be used to visualize starch granule growth rings. It is a fast technique with minimum sample preparation. Compared to SEM and TEM, there is little possibility of artifacts caused by coating, fixation, dehydration, embedding, or sectioning. The pattern of the appearance of growth rings after limited hydrolysis and the loss of granule integrity after extensive hydrolysis may provide insight into the differences in the ultrastructure of starch granules from different sources.

Acknowledgement

This research was funded by a grant (DE-FG02–96ER20234) from The Energy Biosciences Program, the U. S. Department of Energy. *J. H. Li* is also supported by a Post-Doctoral Fellowship from the Natural Sciences and Engineering Research Council of Canada (NSERC). The excellent technical assistance of *Elaine Kunze* and *Susan Magargee* at the Center for Quantitative Cell Analysis, the Pennsylvania State University, is acknowledged.

References

[1] L. E. Fitt, E. M. Snyder: Photomicrographs of starches, in *Starch Chemistry and Technology*, 2nd ed. (Eds. R. L. Whistler, J. N. BeMiller, E. F. Paschall), Academic Press, Orlando, **1984**, p. 675.

[2] A. C. Eliasson, M. Gudmudsson: Starch: Physicochemical and functional aspects, in *Carbohydrates in Food* (Ed. A. C. Eliasson) Marcel Dekker, New York, **1996**.

[3] D. J. Gallant, B. Bouchet, P. M. Baldwin: Microscopy of starch: evidence of a new level of granule organization. *Carbohydr. Polym.* **1997**, *32*, 177–191.

[4] J. H. Li: *Ph. D. Thesis, Physicochemical and structural characterization of hull-less barley starches*, University of Alberta, **2004**.

[5] M. Yamaguchi, K. Kainuma, D. French: Electron microscopic observations of waxy maize starch. *J. Ultrastruct. Res.* **1979**, *69*, 249–261.

[6] A. M. Hermansson, K. Svegmark: Developments in the understanding of starch functionality. *Trends Food Sci. Technol.* **1996**, *7*, 345–353.

[7] P. M. Baldwin, J. Adler, M. C. Davies, C. D. Melia: High resolution imaging of starch granule surfaces by atomic force microscopy. *J. Cereal Sci.* **1998**, *27*, 255–265.

[8] L. Juszczak, T. Fortuna, F. Krok: Non-contact atomic force microscopy of starch granules surface. Part I. Potato and tapioca starches. *Starch/Stärke* **2003**, *55*, 1–7.

[9] J. Szymonska, F. Krok: Potato starch granule nanostructure studied by high resolution non-contact AFM. *Int. J. Biol. Macromol.* **2003**, *33*, 1–7.

[10] A. A. Baker, M. J. Miles, W. Helbert: Internal structure of the starch granule revealed by AFM. *Carbohydr. Res.* **2001**, *330*, 249–256.

[11] M. J. Ridout, M. L. Parker, C. L. Hedley, T. Y. Bogracheva, V. J. Morris: Atomic force microscopy of pea starch granules: granule architecture of wild-type parent, *r* and *rb* single mutants, and the *rrb* double mutant. *Carbohydr. Res.* **2003**, *338*, 2135–2147.

[12] K. C. Huber, J. N. BeMiller: Channels of maize and sorghum starch granules. *Carbohydr. Polym.* **2000**, *41*, 269–276.

[13] M. B. Durrenberger, S. Handschin, B. Conde-Petit, F. Escher: Visualization of food structure by confocal laser scanning microscopy (CLSM). *Lebensm. Wiss. Technol.* **2001**, *34*, 11–17.

[14] F. v. d. Velde, J. v. Riel, R. H. Tromp: Visualisation of starch granule morphologies using confocal scanning laser microscopy (CSLM). *J. Sci. Food Agric.* **2002**, *82*, 1528–1536.

[15] X. Z. Han, B. R. Hamaker: Location of starch granule-associated proteins revealed by confocal laser scanning microscopy. *J. Cereal Sci.* **2002**, *35*, 109–116.

[16] A. Blennow, M. Hansen, A. Schulz, K. Jorgensen, A. M. Donald, J. Sanderson: The molecular deposition of transgenically modified starch in the starch granule as imaged by functional microscopy. *J. Struct. Biol.* **2003**, *143*, 229–241.

[17] D. B. Murphy: *Fundamentals of light microscopy and electronic imaging*, Wiley-Liss, New York, **2001**.

[18] E. M. Snyder: Industrial microscopy of starches, in *Starch Chemistry and Technology*, 2nd ed. (Eds. R. L. Whistler, J. N. BeMiller, E. F. Paschall) Academic Press, Orlando, **1984**, p. 662.

[19] W. Wallace, L. H. Schaefer, J. R. Swedlow: A workingperson's guide to deconvolution in light microscopy. *BioTechniques* **2001**, *31*, 1076–1097.

[20] M. J. Ridout, A. P. Gunning, M. L. Parker, R. H. Wilson, V. J. Morris: Using AFM to image the internal structure of starch granules. *Carbohydr. Polym.* **2002**, *50*, 123–132.

[21] R. Hoover: Acid-treated starches. *Food Rev. Int.* **2000**, *16*, 369–392.

[22] R. G. Rohwer, R. E. Klem: Acid-modified starch: production and uses, in *Starch Chemistry and Technology*, 2nd ed. (Eds. R. L. Whistler, J. N. BeMiller, E. F. Paschall), Academic Press, Orlando, **1984**, p. 530.

(Received: May 31, 2005)
(Revised: September 13, 2005)
(Accepted: September 14, 2005)

